



Discovery of very high energy gamma-ray emission in the W 28 (G6.4–0.1) region, and multiwavelength comparisons

G. ROWELL^{1†}, E. BRION^{2†}, O. REIMER^{3†}, Y. MORIGUCHI⁴, Y. FUKUI⁴, A. DJANNATI-ATAÏ^{5†}, S. FUNK^{3†}

¹ School of Chemistry & Physics, University of Adelaide, Adelaide 5005, Australia

² DAPNIA/DSM/CEA, CE Saclay, F-91191 Gif-sur-Yvette, Cedex, France

³ Stanford University, HEPL & KIPAC, Stanford, CA 94305-4085, USA

⁴ Department of Astrophysics, Nagoya University, Chikusa-ku, Nagoya 464-8602, Japan

⁵ APC, 11 Place Marcelin Berthelot, F-75231 Paris Cedex 05, France

† for the H.E.S.S. Collaboration www.mpi-hd.mpg.de/hfm/HESS

growell@physics.adelaide.edu.au

Abstract: H.E.S.S. observations of the old-age ($>10^4$ yr; $\sim 0.5^\circ$ diameter) composite supernova remnant (SNR) W 28 reveal very high energy (VHE) γ -ray emission situated at its northeastern and southern boundaries. The northeastern VHE source (HESS J1801–233) is in an area where W 28 is interacting with a dense molecular cloud, containing OH masers, local radio and X-ray peaks. The southern VHE sources (HESS J1800–240 with components labelled A, B and C) are found in a region occupied by several HII regions, including the ultracompact HII region W 28A2. Our analysis of NANTEN CO data reveals a dense molecular cloud enveloping this southern region, and our reanalysis of EGRET data reveals MeV/GeV emission centred on HESS J1801–233 and the northeastern interaction region.

Introduction & H.E.S.S. Results

The study of shell-type SNRs at γ -ray energies is motivated by the idea that they are the dominant sites of hadronic Galactic cosmic-ray (CR) acceleration to energies approaching the *knee* ($\sim 10^{15}$ eV) and beyond, e.g. [1]. Gamma-ray production from the interaction of these CRs with ambient matter and/or electromagnetic fields is a tracer of such particle acceleration, and establishing the hadronic or electronic nature of the parent CRs in any γ -ray source is a key issue.

W 28 (G6.4–0.1) is a composite or mixed-morphology SNR, with dimensions $50' \times 45'$ and an estimated distance between 1.8 and 3.3 kpc (eg. [2, 3]). It is an old-age SNR (age 3.5×10^4 to 15×10^4 yr [4]), thought to have entered its radiative phase of evolution [3]. The shell-like radio emission [5, 6] peaks at the northern and northeastern boundaries where interaction with a molecular cloud [7] is established [8, 9]. The X-ray emission, which overall is well-explained by a ther-

mal model, peaks in the SNR centre but has local enhancements in the northeastern SNR/molecular cloud interaction region [10]. Additional SNRs in the vicinity of W 28 have also been identified: G6.67–0.42 and G7.06–0.12 [11]. The pulsar PSR J1801–23 with spin-down luminosity $\dot{E} \sim 6.2 \times 10^{34}$ erg s⁻¹ and distance $d \geq 9.4$ kpc [12], is at the northern radio edge.

Given its interaction with a molecular cloud, W 28 is an ideal target for VHE observations. This interaction is traced by the high concentration of 1720 MHz OH masers [13, 14, 15], and also the location of very high-density ($n > 10^3$ cm⁻³) shocked gas [9, 8]. Previous observations of the W 28 region at VHE energies by the CANGAROO-I telescope revealed no evidence for such emission [16] from this and nearby regions.

The High Energy Stereoscopic System (H.E.S.S.: see [17] for details and performance) has observed the W 28 region over the 2004, 2005 and 2006 seasons. After quality selection, a total of ~ 42 hr observations were available for analysis.

Data were analysed using the moment-based Hillas analysis procedure employing *hard cuts* (image size >200 p.e.), the same used in the analysis of the inner Galactic Plane Scan datasets [18, 19]. An energy threshold of ~ 320 GeV results from this analysis. The VHE γ -ray image in Fig. 1 shows that two source of VHE γ -ray emission are located at the northeastern and southern boundaries of W 28. The VHE sources are labelled HESS J1801–233 and HESS J1801–240 where the latter can be further subdivided into three components A, B, and C. The excess significances of both sources exceed $\sim 8\sigma$ after integrating events within their fitted, arcminute-scale sizes. Similar results were also obtained using an alternative analysis [20].

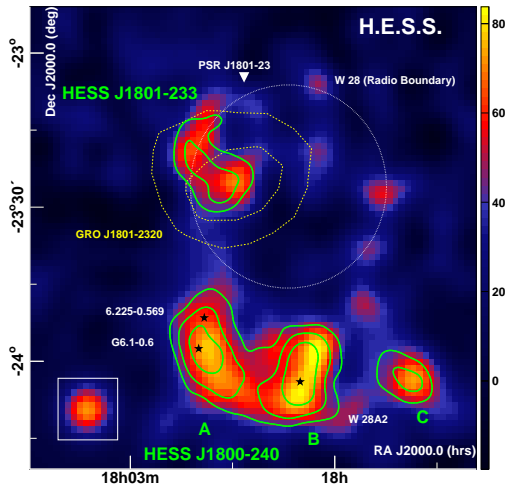


Figure 1: H.E.S.S. VHE γ -ray excess counts, corrected for exposure and Gaussian smoothed (with $4.2'$ std. dev.). Green contours — VHE 4, 5, and 6σ significance for an integrating radius $\theta=0.1^\circ$. Thin-dashed circle — approximate radio boundary of the SNR W 28. Additional objects: HII regions (black stars); W 28A2, G6.1–0.6 6.225–0.569; Thick-dashed yellow lines — 68% and 95% location contours of GRO J1801–2320; White trigangle — PSR J1801–23. Inset — pointlike source under identical analysis and smoothing as for the main image.

W 28: The Multiwavelength View

We have revisited EGRET MeV/GeV data, including data from the CGRO observation cycles (OC) 1 to 6, which slightly expands on the dataset of the 3rd EGRET catalogue (using OCs 1 to 4; [21], revealing the source 3EG J1800–2338. We find a pointlike $E > 100$ MeV source in the W 28 region, labelled GRO J1801–2320 in Fig 1. The 68% and 95% location contours of GRO J1801–2320 match well the location of HESS J1801–233. However we cannot rule out a connection to HESS J1800–240 due to the degree-scale EGRET PSF.

Fig. 2 presents ^{12}CO ($J=1-0$) observations from the NANTEN Galactic Plane survey [22] covering the line-of-sight velocity ranges $V_{\text{LSR}} = 0$ to 10 km s^{-1} and 10 to 20 km s^{-1} . These ranges represent distances 0 to ~ 2.5 kpc and 2.5 to ~ 4 kpc respectively and encompass the distance estimates for W 28. We cannot rule out however, distances ~ 4 kpc for the $V_{\text{LSR}} > 10 \text{ km s}^{-1}$ cloud components. It is clear that molecular clouds coincide well with the VHE sources. The northeastern cloud $V_{\text{LSR}} < 10 \text{ km s}^{-1}$ component near HESS J1801–233, is already well-studied [8, 9]. Contributions from the $V_{\text{LSR}} > 10 \text{ km s}^{-1}$ cloud components are also likely. The molecular cloud to the south of W 28 coincides well with HESS J1800–240 and its three VHE components. The $V_{\text{LSR}} < 10 \text{ km s}^{-1}$ component of this cloud coincides well with HESS J1800–240B, and may represent the dense molecular matter surrounding the ultra-compact HII region W 28A2. This cloud also extends to $V_{\text{LSR}} \sim 20 \text{ km s}^{-1}$ and thus, similar to HESS J1801–233, the total VHE emission in HESS J1800–240 may result from several molecular cloud components in projection.

Fig. 3 compares the radio (left panel — VLA 90 cm [23]), infrared and X-ray views (right panel MSX $8.28 \mu\text{m}$ and ROSAT PSPC 0.5 to 2.4 keV [10]) with the VHE results. HESS J1801–233 overlaps the northeastern shell of the SNR, coinciding with a strong peak in the 90 cm continuum emission. Additional SNRs G6.67–0.42 and G7.06–0.12 [11, 24] are indicated. The non-thermal radio arc G5.71–0.08 is a SNR candidate [23], and is possibly a counterpart to HESS J1801–240C. is positioned within 0.1° of

the centroid of HESS J1800–240B. W 28A2, at a distance $d \sim 2$ kpc, exhibits energetic bipolar molecular outflows [25, 26, 27] and may therefore be an energy source for particle acceleration in the region. The other HII regions G6.1–0.6 [28] and 6.225–0.569 [29] are also associated with radio emission.

The X-ray morphology (Fig. 3 right panel) shows the central concentration of X-ray emission. A local X-ray peak or *Ear* is seen at the northeastern W 28 boundary. The HII regions, W 28A2 and G6.1–0.6 are prominent in the MSX 8.28 μm image (Fig. 3 right panel), indicating that a high concentration of heated dust still surrounds these very young stellar objects.

Discussion and Conclusions

H.E.S.S. and NANTEN observations reveal VHE emission in the W 28 region spatially coincident with molecular clouds. The VHE emission and molecular clouds are found at the northeastern boundary, and $\sim 0.5^\circ$ south of W 28 respectively. The SNR W 28 may be a source of power for the VHE sources, although there are additional potential particle accelerators in the region such as other SNR/SNR-candidates, HII regions and open clusters. Further details concerning these results and discussion are presented in [30].

Acknowledgements

The support of the Namibian authorities and of the University of Namibia in facilitating the construction and operation of H.E.S.S. is gratefully acknowledged, as is the support by the German Ministry for Education and Research (BMBF), the Max Planck Society, the French Ministry for Research, the CNRS-IN2P3 and the Astroparticle Interdisciplinary Programme of the CNRS, the U.K. Particle Physics and Astronomy Research Council (PPARC), the IPNP of the Charles University, the Polish Ministry of Science and Higher Education, the South African Department of Science and Technology and National Research Foundation, and by the University of Namibia. We appreciate the excellent work of the technical support staff in Berlin, Durham, Hamburg, Heidelberg, Palaiseau,

Paris, Saclay, and in Namibia in the construction and operation of the equipment. The NANTEN project is financially supported from JSPS (Japan Society for the Promotion of Science) Core-to-Core Program, MEXT Grant-in-Aid for Scientific Research on Priority Areas, and SORST-JST (Solution Oriented Research for Science and Technology: Japan Science and Technology Agency). We also thank Crystal Brogan for the VLA 90 cm image.

References

- [1] G. V.L., S. Syrovatskii, *The Origin of Cosmic Rays*, (New York: Macmillan), 1964.
- [2] G. C., *Ap&SS* 40 (1976) 91.
- [3] L. T.A., *Sov. Astron. Lett.* 7 (1981) 17.
- [4] K. V. et al., *ApJ* 409 (1993) L57.
- [5] L. K. et al., *ApJ* 373 (1991) 567.
- [6] D. G. et al., *AJ* 120 (2000) 1933.
- [7] W. A., *ApJ* 245 (1981) 105.
- [8] R. W. et al., *ApJ* 618 (2005) 297.
- [9] A. Y. et al., *PASJ* 51 (1999) L7.
- [10] R. J. et al., *ApJ* 575 (2002) 201.
- [11] Y.-Z. F. et al., *ApJ* 540 (2000) 842.
- [12] C. M. et al., *ApJ* 580 (2002) 909.
- [13] F. D. et al., *ApJ* 424 (1994) L111.
- [14] C. M. et al., *ApJ* 489 (1997) 143.
- [15] C. M. et al., *ApJ* 522 (1999) 349.
- [16] R. G. et al., *A&A* 359 (2000) 337.
- [17] H. J.A., *New Astron. Rev.* 48 (2004) 331.
- [18] A. F. et al., *Science* 307 (2005) 1938.
- [19] A. F. et al., *ApJ* 636 (2006) 777.
- [20] de Naurois M., *arXiv:astro-ph/0607247*.
- [21] H. R. et al., *ApJS* 123 (1999) 79.
- [22] M. K. et al., *PASJ* 53 (2001) 1003.
- [23] B. C. et al., *ApJ* 639 (2006) L25.
- [24] H. D. et al., *AJ* 131 (2006) 2525.
- [25] H. P. et al., *A&A* 197 (1988) L19.
- [26] A. J. et al., *ApJ* 475 (1997) 693.
- [27] S. P. et al., *ApJ* 616 (2004) L35.
- [28] K. T. et al., *ApJ* 488 (1997) 224.
- [29] L. F.J., *ApJ (Supp)* 71 (1989) 469.
- [30] A. F. et al., *A&A* submitted.

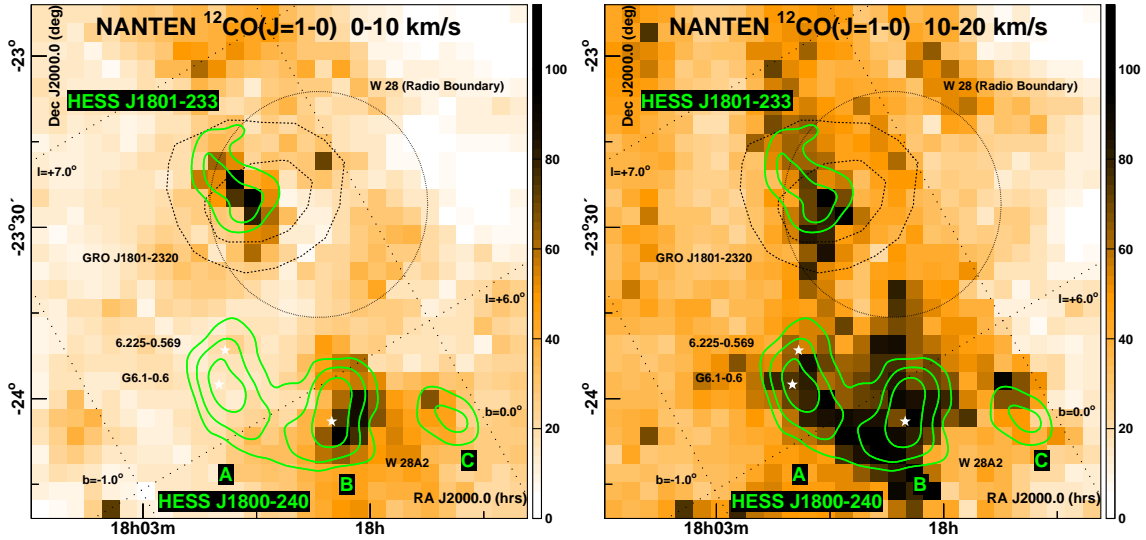


Figure 2: **Left:** NANTEN $^{12}\text{CO}(J=1-0)$ image (linear scale in K km s^{-1}) for $V_{\text{LSR}}=0$ to 10 km s^{-1} with VHE γ -ray significance contours overlaid (green) — levels $4, 5, 6\sigma$ and other features as in Fig. 1. **Right:** NANTEN $^{12}\text{CO}(J=1-0)$ image for $V_{\text{LSR}}=10$ to 20 km s^{-1} (linear scale and same maximum as for left panel).

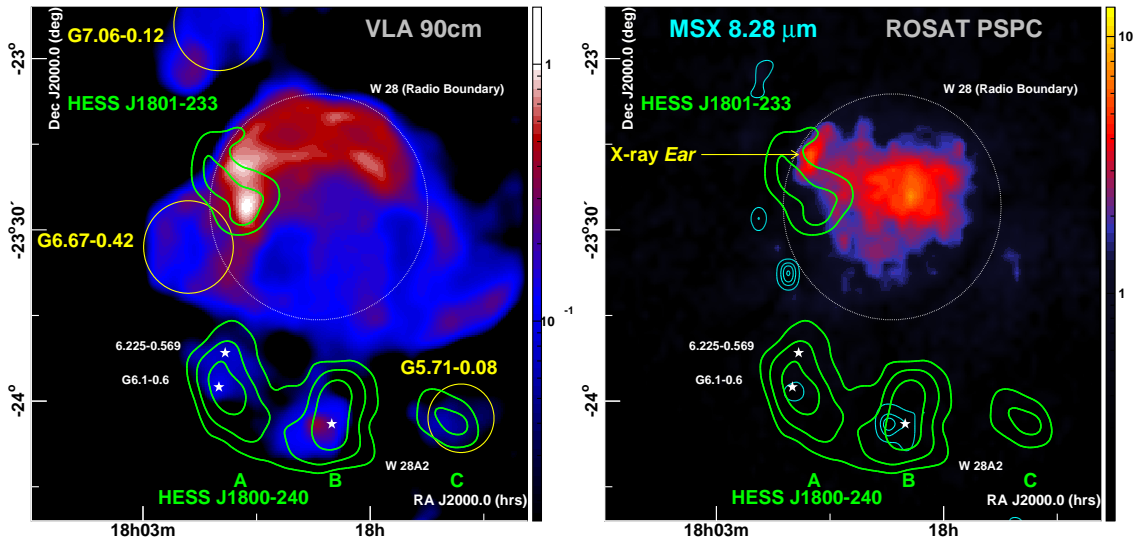


Figure 3: **Left:** VLA 90cm radio image [23] in Jy beam^{-1} . The VHE significance contours (green) from Fig. 1 are overlaid along with the HII regions (white stars) and the additional SNRs and SNR candidates (with yellow circles indicating their location and approximate dimensions) discussed in text. **Right:** ROSAT PSPC image — 0.5 to 2.4 keV (smoothed counts per bin [10]). Overlaid are contours (cyan — 10 linear levels up to $5 \times 10^{-4} \text{ W m}^{-2} \text{ sr}^{-1}$) from the MSX 8.28 μm image. Other contours and objects are as for the left panel. The X-ray *Ear* representing a peak at the northeastern edge is indicated.